Eco-Environment & Health 2 (2023) 32–39

Contents lists available at ScienceDirect

Eco-Environment & Health

journal homepage: www.journals.elsevier.com/eco-environment-and-health

Original Research Article

Bidirectional role of synthetic musk tonalide as photosensitizer and activator on amino acids: Formation of sensitizer imine at aqueous chemistry interface of skin

Na Luo [a,b], Yanpeng Gao [a,b], Mei Wang [a,b], Xiaolin Niu [a,b], Guiying Li [a,b], Taicheng An [a,b,*]

[a] Guangdong-Hong Kong-Macao Joint Laboratory for Contaminants Exposure and Health, Guangdong Key Laboratory of Environmental Catalysis and Health Risk Control, Institute of Environmental Health and Pollution Control, Guangdong University of Technology, Guangzhou 510006, China
[b] Guangzhou Key Laboratory of Environmental Catalysis and Pollution Control, Key Laboratory of City Cluster Environmental Safety and Green Development of the Ministry of Education, School of Environmental Science and Engineering, Guangdong University of Technology, Guangzhou 510006, China

ARTICLE INFO

Keywords:
Personal care products
Amino acids
Photosensitive damage
Electron transfer
Imines

ABSTRACT

Personal care products (PCPs) inevitably come into contact with the skin in people's daily life, potentially causing adverse effects on human health. The adverse effects can be exacerbated under UV irradiation but are rarely studied. In this study, to clearly understand the damage of representative PCPs to human skin and their photochemical transformation behaviors, fragrance tonalide (AHTN) was measured in the presence of amino acids as a basic building block of human tissue. The results showed that amino acids could decelerate the photochemical transformation rate of AHTN, increasing the likelihood of AHNT persisting on the skin surface and the health risk to the human being. Further, the interaction between amino acids and AHTN was investigated. AHTN could play bidirectional roles in damaging amino acids: the photosensitizer and reactive activator. As a photosensitizer, the $^1O_2$ generated from the AHTN photosensitization was partly employed to oxidative damage amino acids. Furthermore, by combining experiments with quantum chemical computation, the carbonyl group of the activator AHTN was found to be the active site to activate the N-containing group of amino acids. The activation mechanism was the electron transfer between AHTN and amino acids. Imines formed during the photochemical transformation of AHTN with histidine/glycine were the molecular initiating event for potential skin sensitization. This study reported for the first time that skin photosensitizer formation threatens human health during the photochemical transformation of AHTN.

1. Introduction

In recent years, a large number of personal care products (PCPs) have been developed to improve human living standards [1,2]. However, ingredients of PCPs inevitably come into contact directly with human skin and easily remain on the skin surface during long-term daily use [3,4]. Especially when the skin is overexposed to UV, these residual additives on the skin surface can act as photosensitizers to damage the skin cells [5–7], resulting in skin aging, pigmentation, inflammation, and even the formation of tumors [8,9]. Therefore, the excessive use of these PCPs might severely affect human skin health [10]. As known, skin photosensitization includes many biological events involving thousands of proteins [11]. Skin photosensitization begins with a chemical event identified modification of amino acid residues in proteins [12]. Exploring the chemical modification processes of these amino acid residues by PCP additives will reveal the potentially photosensitive components. Besides, amino acids are considered the basic building blocks of life because they can form various needed proteins [13,14]. Thus, investigating the chemical modification mechanism in PCP additives on these basic units of life will help us fundamentally understand the photosensitive effect.

Synthetic musks, as a group of representative PCPs additives, are widely used in cosmetics, perfumes, body lotions, essential oil, toiletries, antiperspirants, soaps, and shampoo [15,16]. The annual use of these scented products is as high as 10,000 tons globally [17]. In particular, in the current market, polycyclic and nitro-musks are the two most commonly used synthetic musks. However, due to their photosensitivity [18–20], carcinogenicity [21–23], and endocrine-disrupting effects [24], nitro-musks have significantly been restricted in many countries since the late 20th century [25]. As a result, with the drastically decreasing production of nitro-musks, polycyclic musks became the alternative

* Corresponding author.
E-mail address: antc99@gdut.edu.cn (T. An).

https://doi.org/10.1016/j.eehl.2023.03.002
Received 2 November 2022; Received in revised form 23 February 2023; Accepted 1 March 2023
Available online 10 March 2023

fragrances and were listed as one of the high-yield chemicals by the United States Environmental Protection Agency [26].

Unfortunately, increasing research reported that polycyclic musks have strong bioaccumulation and endocrine-disrupting effects [27] and can interfere with organisms' growth, development, and metabolism [28–30]. Furthermore, as the report on the inhibition of the activity of multidrug efflux transporters responsible for multixenobiotic resistance indicated, the adverse effects of polycyclic musks as efflux transporter chemosensitizers could be very severe [31]. Additionally, our early research revealed that polycyclic musks could cause photo-induced oxidative damage to dissolved free amino acids [32]. In other words, residual tonalide (AHTN) on the skin surface could destroy critical biomolecules, such as proteins and enzymes, because their basic building blocks were amino acids [33], indicating the potential for skin sensitization damage.

Chemical sensitizers usually trigger covalent binding with amino acids to initiate skin sensitization, leading to skin diseases, such as allergic contact dermatitis [34]. The formation of this covalent adduct is considered to be the critical molecular initiating event (MIE) of the adverse outcome pathway (AOP) [35]. Although it is unclear whether synthetic musks could induce skin allergy, the typical aldehydes and ketones structure might also cause amino acid sensitization damage [12], suggesting that synthetic musks may trigger MIE for AOP at the aqueous interface of skin. However, relevant researches are still very scarce. Especially under ultraviolet irradiation, the photosensitization potential and mechanism of the residual synthetic musks on the skin surface during the photochemical transformation are unclear. Identifying potential skin sensitizers in PCPs additives as soon as possible is significant for reducing human health hazards.

The main objectives of this work were to explore the potential skin photosensitization interaction mechanism of typical polycyclic musk, AHTN. Previous research showed that PCP additives could easily enter the skin surface by dissolving in body fluids, further influencing human health [36]. Thus, the aqueous chemistry interface of skin (water and acetonitrile for 1:1) was designed to simulate the reaction, which has been successfully applied to study the photosensitization mechanism of other skin photosensitizers, such as isoeugenol, benzaldehyde, and glutaraldehyde [34,37,38]. Glycine (Gly), the simplest amino acid, can serve as a typical model for mechanism investigation. Besides, according to our previous work, histidine (His) and methionine (Met) with non-absorbing sunlight have the highest reactivity in both acidic and alkaline solutions [32]. Therefore, His, Gly, and Met were selected as the model to investigate the mechanism. Firstly, the photochemical transformation kinetics of AHTN were measured in different concentrations of different amino acids (His, Gly, and Met). Secondly, the interaction mechanism between AHTN and amino acids was attempted from direct and indirect photochemical transformation pathways via both experimental and computational methods. Finally, the effects of amino acids on the photochemical transformation products of AHTN were also analyzed, and the imines were identified using high-performance liquid chromatography quadrupole-time of flight tandem mass spectrometry. This study provided a scientific basis for understanding the reaction mechanism of AHTN with key small biological molecules and determining the photochemical toxic reaction mechanism of AHTN on the skin surface.

2. Materials and methods

2.1. Chemicals

AHTN (7-acetyl-1,1,3,4,4,6-hexamethyl-tetrahydronaphtalene) was purchased from Adamas Reagent Ltd. (Shanghai, China) with purity >98%. Amino acids, including L-histidine (His, 99%), L-glycine (Gly, 99%), and L-methionine (Met, 99%), were from Macklin Biochemical Co., Ltd. (Shanghai, China). Potassium dihydrogen phosphate (KH_2PO_4, 99%) and dipotassium phosphate (K_2HPO_4, 99%) were analytical grade reagents purchased from Guangzhou Chemical Reagent Factory (Guangzhou, China). Text S1 in the Supporting Information (SI) summarized other reagents used in this work. All reagents and solvents were used as received, and all solutions were prepared with ultrapure water (Resistivity = 18.25 MΩ cm).

2.2. Photochemical transformation experiments

AHTN and amino acids mixture solution were primarily prepared in acetonitrile : H_2O (1:1). The buffer solution with a concentration of 2.5 mM was prepared in ultrapure water with the addition of KH_2PO_4–K_2HPO_4 (pH = 4.5−8.5). The reaction solution was approximately 25 mL, and a high-pressure mercury lamp (Bilon, Inc., Shanghai, China) was surrounded by a 290 nm cut-off filter. Furfuryl alcohol (FFA) was selected as the probe of singlet oxygen, and rose bengal (RB) was employed as the singlet oxygen photosensitizer [39]. Nitro-blue tetrazolium (NBT) was selected as a probe to explore electron transfer reaction on the photochemical transformation of AHTN with or without amino acids, which could be reduced to form NBT^+, resulting that the absorbance of the mixtures increased at 560 nm [40]. Detailed photochemical procedures are provided in Text S2 in SI. The glassware was rinsed with pure water and heated to 450 °C to avoid sample contamination. Procedural blanks were set with solvent (ultrapure water and acetonitrile 1:1) to eliminate background in the analyses. All experiments were set three times parallel, and results were expressed as average ± SD. Statistical significance was analyzed using one-way ANOVA. The p-values <0.05 represented the significance level.

All the sample was monitored using a high-performance liquid chromatograph with a photodiode array detector (Agilent 1260 HPLC) equipped with Zorbax XDB C_{18} column (5 μm, 4.6 × 150 mm). The imines and photochemical transformation by-products of AHTN were identified using HPLC-TOF-MS (Agilent 1290 HPLC and G6545B) equipped with Agilent Eclipse Plus C_{18} column (1.78 μm, 2.1 × 50 mm) at 1 mL/min eluent flow rate. Detailed detection methods are described in Text S3 in SI.

2.3. Computational methods

All quantum chemical calculations in this work were carried out using the Gaussian 09 package. The reaction system was simulated using the self-consistent reaction field (SCRF) method by using water as the solvent. The geometry optimization of atoms was performed using a 062x/6-311G** basis set. Multiwfn optimized the ADCH atomic charges of each amino acid. Density functional theory (DFT) was employed to investigate the reaction interaction energy of AHTN and its transformation products with amino acids using the functional Mm062x method with a 6-311G** basis set. The electron energy was obtained by structure optimization, and the heat of the reaction was also calculated by subtracting the product energy from the reactant energy.

2.4. Determination of $f_{^1O_2}$ and $k_{^1O_2}$

The furfuryl alcohol was employed as $^1O_2$ probe. And the fraction of $^1O_2$ ($f_{^1O_2}$) available for the reaction with AHTN or amino acids in this system can be expressed as Eq. 1.

$$f_{^1O_2,AHTN} = \frac{k_{^1O_2,AHTN}[AHTN]}{k_{^1O_2,sol} + k_{^1O_2,AHTN}[AHTN] + k_{^1O_2,amino\ acid}[amino\ acid]} \quad (1)$$

where [AHTN] and [amino acid] represented the concentrations of AHTN and amino acid, and $k_{^1O_2,\ AHTN}$ and $k_{^1O_2,\ amino\ acid}$ were the bimolecular reaction rate constants of AHTN and amino acid with $^1O_2$, respectively. The values of $k_{^1O_2,\ His}$ and $k_{^1O_2,\ Met}$ were 9×10^7 and 1.7×10^7 M^{-1} s^{-1}, respectively [41]. The physical quenching of $^1O_2$ by solvent (solvent, ACN : H_2O = 1:1), $k_{^1O_2,\ sol}$, is 6.7×10^4 s^{-1} [42].

The $k_{^1O_2,\ AHTN}$ could be calculated by Eq. 2.

$$ln\left(\frac{[FFA]_t}{[FFA]_0}\right) = \frac{k_{^1O_2,FFA}}{k_{^1O_2,AHTN}} ln\left(\frac{[AHTN]_t}{[AHTN]_0}\right) \quad (2)$$

where $[FFA]_t$ and $[FFA]_0$ were the concentration of FFA at time zero and time t (min), and the bimolecular reaction rate constants of FFA and $^1O_2$ ($k_{^1O_2,\ FFA}$) were 1.2×10^8 [43].

3. Results and discussion

3.1. Kinetics and by-products identified during the photochemical transformation of AHTN in the presence of amino acids

AHTN (500 μM) could be photochemically degraded completely within 25 min under UV irradiation (Fig. 1), and the degradation kinetics curves of AHTN were confirmed to the pseudo-first-order kinetic equation with the rate constant of 8.4×10^{-2} min^{-1} ($R^2 = 0.99$) (Fig. 1D). However, the photochemical degradation rate constants of AHTN decreased to $(4.8–7.4) \times 10^{-2}$, $(5.5–7.6) \times 10^{-2}$, and $(5.6–7.6) \times 10^{-2}$ min^{-1} in the presence of 5–500 μM His, Gly, and Met, respectively (Fig. 1D). Figure 1D summarizes the photochemical degradation rate constants of AHTN in the presence of amino acids (0, 5, 50, 250, and 500 μM), and the rate constant of AHTN without amino acids was significantly higher than those in the presence of amino acids. Besides, these rate constants of AHTN decreased with increasing amino acid concentration. The photochemical degradation curves of AHTN between the groups showed significant differences (Fig. 1A–C). In other words, amino acids could inhibit the photochemical transformation of AHTN and enhanced inhibition occurs with increasing concentration of amino acids.

It is well known that photochemical transformation is one of the detoxification pathways of PCPs additives [44]. The reduction of the AHTN photochemical transformation rate indicated a prolonged detoxification time, which increased the residual time of AHTN on the human skin surface and raised the health risk to the human being. Meanwhile, it should be noted that amino acids in solution could also be continuously degraded during the photochemical transformation of AHTN, and approximately 20% amino acids (500 μM) were consumed when AHTN was utterly eliminated within 25 min (Fig. S1). Besides, the control experiments were set up for comparison, which showed that amino acids were undegraded without AHTN. These results were consistent with a previous study on synthetic musks-mediated amino acid damage [32]. In other words, AHTN could induce photosensitive damage to amino acids while slowing down the photochemical transformation of AHTN itself. This photosensitization effect could damage human skin through photoaging and photoallergy [45]. Therefore, exploring the interaction mechanism between AHTN and amino acids in the photochemical system could reveal the potential adverse effects of AHTN photosensitization on human skin.

To clarify the interaction mechanism between AHTN and amino acids, the influence of amino acids on the photochemical transformation products of AHTN would need to be investigated because the formation of by-products could directly depend on the transformation mechanism of AHTN [46]. Based on the retention time of chromatographic separation, eight by-products from AHTN photochemical transformation were labeled as P1–P8, which were formed in the absence of amino acids (Table S1 and Fig. S2). Moreover, according to the transformation processes of AHTN, P5 and P6 appeared as first-generation by-products; correspondingly, P1–P4, P7, and P8 were the second-generation by-products formed from the first-generation by-products [46]. The MS/MS figures of P1–P8 are shown in Fig. S3. Unexpectedly, in addition to these eight by-products, the HPLC-TOF-MS analysis in the presence of His or Gly revealed the presence of new peaks with larger molecular mass than that of AHTN and amino acids, and these by-products were named $N_{His}1-N_{His}3$ and $N_{Gly}1-N_{Gly}2$, respectively (Fig. 2). It was likely that the

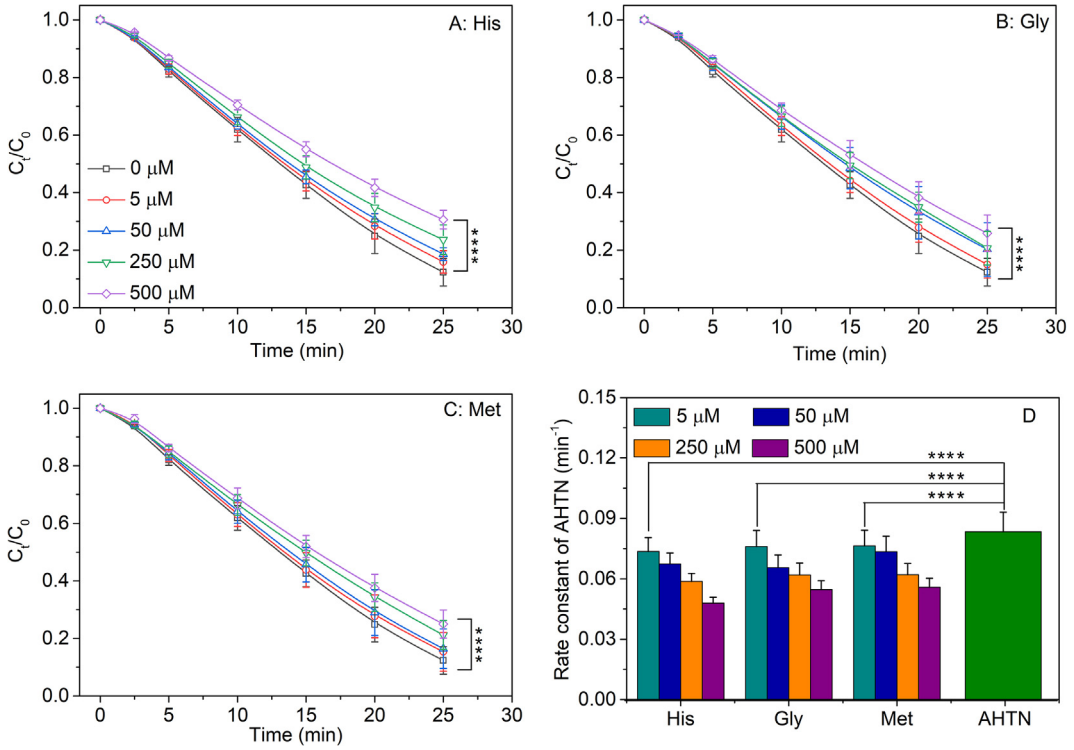

Fig. 1. The photochemical degradation kinetic curves (A, B, and C) and rate constant (D) of AHTN at different concentrations of amino acids. The concentration of AHTN was 500 μM, and these legends showed the concentration of amino acid (0, 5, 50, 250, and 500 μM). Data were means of three replicates and analyzed statistically with one-way ANOVA. Statistical significance between the groups is indicated as ****$p < 0.0001$.

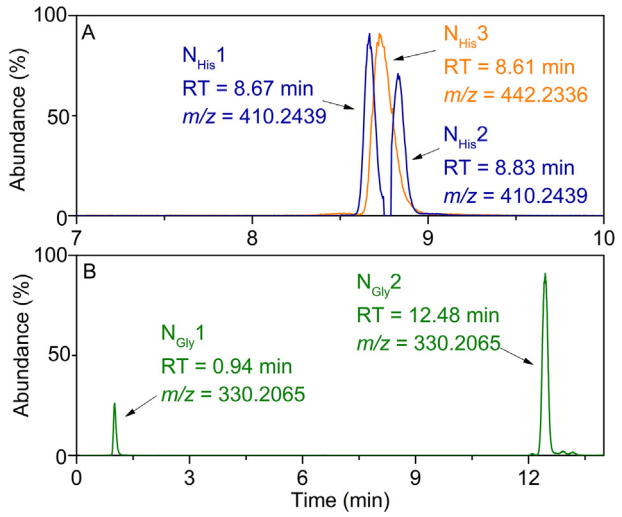

Fig. 2. The extraction of ion chromatogram of imine compounds detected in the photochemical transformation solution of AHTN with His (A) and Gly (B).

macromolecular adducts were formed by inducing the distortion of amino acids during the photochemical transformation of AHTN, potentially inducing skin sensitization. This similar phenomenon has been reported in typical skin sensitizers isothiazolinone, which can react significantly with amino acid side chains and lead to binding to form macromolecules [47]. Therefore, the identification of these new by-products ($N_{His}1-N_{His}3$ and $N_{Gly}1-N_{Gly}2$) was carried out first. Table S2 summarizes the values of *m/z*, molecular formulas, predicted structures, and the corresponding mass errors of these products, as well as their confidence levels according to the scales established by Schymanski et al. [48]. The MS/MS of these new by-products ($N_{His}1-N_{His}3$ and $N_{Gly}1-N_{Gly}2$) are provided in Fig. 3 and Fig. S4. The identification of by-products ($N_{His}1-N_{His}3$ and $N_{Gly}1-N_{Gly}2$) belonged to level 3 of the confidence level. Analyzing the accurate *m/z* of the by-products could predict their precise molecular formulas through Agilent software of qualitative navigator. The difference between the predicted and measured *m/z* was less than 5 ppm, supporting their tentative identification.

By-products $N_{His}1$ and $N_{His}2$ showed the same measured mass as *m/z* 410.2426 ($[M+H]^+$, mass error: −0.14 for $N_{His}1$ and −0.11 for $N_{His}2$), indicating that they are isomers and a predicted molecular formula $C_{24}H_{31}N_3O_3$. As Fig. 3 and Fig. S4 show, the mass difference between *m/z* = 410.2426 (mass error: −0.14) and the fragment *m/z* = 255.1741 (mass error: 0.24) was 155.0685, corresponding to the loss of a neutral molecule of His (predicted mass: 155.0695). Besides, the initial fragmentation pattern of *m/z* = 410.2426 (mass error: −0.14) was consistent with that of His standard substance, described minutely in Text S4. Its fragment *m/z* = 255.1741 (mass error: 0.24) matched well with the fragment of first-generation by-product P5 (Fig. S5), which was formed during AHTN photochemical transformation in the absence of His. Based on the MS/MS fragment information and mass loss of His and P5, it was reasonable to confirm that $N_{His}1$ was the adduct of His with P5. That is, $N_{His}1$ was obtained by removing H_2O from P5 (measured mass: 272.1776, mass error: 0.19) combined with His (measured mass:155.0695, mass error: −1.24), considered to be an imine. Similarly, $N_{His}2$ was the bonding of His with P6 based on molecular ions and the corresponding fragment ions, and P6 was also the first-generation by-product produced during AHTN photochemical transformation without His (Text S4) [46]. By-product $N_{His}3$, with a measured mass of 442.2331 ($[M+H]^+$, mass error: −2.55), was predicted as $C_{24}H_{31}N_3O_5$ (predicted mass: 441.2264). The *m/z* difference between $N_{His}3$ and $N_{His}1$ was 31.9899, matching the predicted mass of O_2 (predicted mass: 31.9898). These data indicated that $N_{His}3$ could be the oxidation by-product of $N_{His}1$. Figure 3C shows that the mass difference between $N_{His}3$

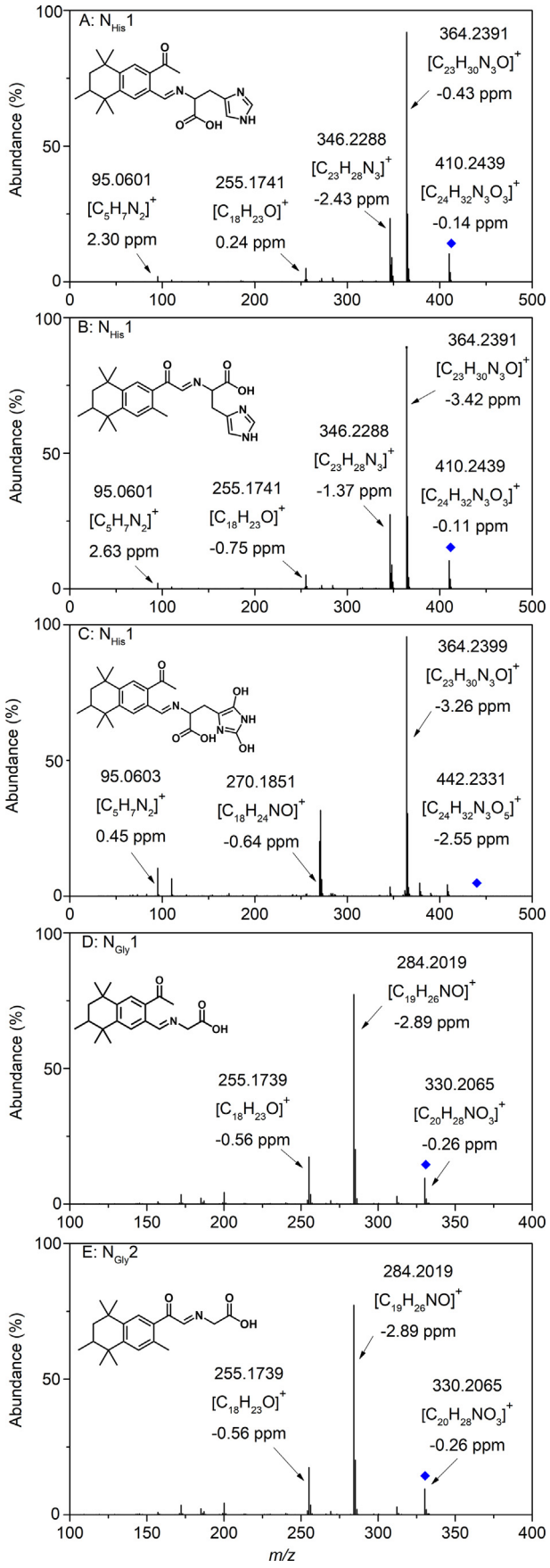

Fig. 3. MS/MS of imine compounds detected in the photochemical transformation of AHTN with His (A–C) and Gly (D–E).

(measured mass: 442.2331, mass error: −2.55) and m/z = 408.2283 (mass error: −1.25) fragment was 34.0048, corresponding to the simultaneous loss of two hydroxyls (predicted mass: 34.0055). A neutral group CH_2O_2 (predicted mass: 46.0055) was left further to form the fragment of m/z = 364.2399 (mass error: −3.26). Moreover, m/z = 364.2399 (mass error: −3.26) fragment featured two pieces with m/z of 270.1854 (mass error: −0.64) and 95.0603 (mass error: 0.45), inducing from the cracking process of m/z = 364.2399 (mass error: −3.26) could be the C–N bond breaking because the predicted molecular of m/z = 270.1854 of $C_{18}H_{23}NO$ and the His fragment ion m/z = 95.0603 (Text S4). Therefore, we confirmed that the by-product $N_{His}3$ (Table S2) was formed via the oxidation of the imidazole group in $N_{His}1$.

Similarly, $N_{Gly}1$ and $N_{Gly}2$ also had the same measured mass as m/z 330.2072 ($[M+H]^+$, mass error: −0.26), indicating that they are isomers and the predicted molecular formula $C_{20}H_{27}NO_3$. As Fig. 3 shows, $N_{Gly}1$ and $N_{Gly}2$ would lose the neutral group CH_2O_2 (predicted mass: 46.0055) to form the fragment of m/z = 284.2019 (mass error: −2.89) after rearrangement and cracking. The mass difference between m/z = 330.2072 (mass error: 0.26) and m/z = 255.1741 (mass error: −0.56) was 75.0331, corresponding to the loss of a neutral molecule of Gly (predicted mass: 75.0320). Hence, $N_{Gly}1$ and $N_{Gly}2$ were generated by removing H_2O from P5 and P6 combined with Gly to form the imine structure, respectively.

Therefore, the above data analysis indicates that these photochemical transformation by-products of AHTN could adduct amino acids to form imines. Furthermore, the presence of amino acids could affect the generation of by-products P1–P8 (Fig. S6). For example, the formation of products P1 and P3 was promoted by His and Gly, while products P2, P7, and P8 were inhibited by His and Met, and P4 vanished in the presence of His. Moreover, based on the transformation mechanism of AHTN in the absence of amino acids (Text S5 and Fig. S7), AHTN absorbed photon energy to form a singlet state and then an excited triplet state. The excited triplet state of AHTN would transfer its power to O_2 to form $^1O_2$ and undergo intramolecular electron transfer to form biradicals [46]. Therefore, these two components, $^1O_2$ and biradicals, affected the photochemical transformation of AHTN regardless of the presence of amino acids. We could infer from the above results that AHTN could be a photosensitizer to produce $^1O_2$ to oxidize these three amino acids and act as an activator to induce electron transfer, potentially forming imines during the photochemical transformation of AHTN, further damaging human skin.

3.2. The bidirectional role of photosensitized AHTN in the presence of amino acids: photosensitizer and activator

3.2.1. Photosensitizer

EPR signals of $^1O_2$ generated during the photochemical transformation of AHTN at different periods were studied (Fig. S8). The result indicated that $^1O_2$ could be continuously produced during the photochemical transformation of AHTN. Therefore, this complex system could stabilize photosensitive amino acids via $^1O_2$ oxidation. However, $^1O_2$ could both be an oxidant to damage amino acids and be used to promote the self-sensitization of AHTN, suggesting the competition of $^1O_2$ to reduce the degradation rate of AHTN [32,41]. Therefore, the $^1O_2$ produced in the composite system was incompletely used to oxidize amino acids, inducing us to study the fraction of $^1O_2$ ($f_{^1O_2}$) available for the reaction with AHTN or amino acids in this system to confirm the photosensitivity of AHTN to amino acids via $^1O_2$ oxidation, as expressed by Eq. 1. And the bimolecular reaction rates of AHTN and $^1O_2$ ($k_{^1O_2,\ AHTN}$) could be calculated by Eq. 2.

According to the experimental determination and calculation of the above equations, $k_{^1O_2,\ AHTN}$ equaled 3.1 × 10^7 M^{-1} s^{-1} as listed in Table S3. Furthermore, in the presence of His, the values of $f_{^1O_2,\ AHTN}$ and $f_{^1O_2,\ His}$ were calculated as 25.6% and 74.3%, respectively. Hence, 74.3% of $^1O_2$ generated from AHTN photochemical transformation would be used for His oxidative damage, while the rest of 25.6% $^1O_2$ could oxidize photosensitizer AHTN. Similarly, approximately 35% of $^1O_2$ would be utilized for Met oxidative damage in the presence of Met, and the rest could oxidize AHTN. It had been reported that Gly could not react with $^1O_2$ [41], so we will not discuss this further. The fractions of $^1O_2$ ($f_{^1O_2}$) available for the reaction with AHTN or amino acids were calculated and are summarized in Table S3.

Overall, AHTN, as a photosensitizer, could produce $^1O_2$ from the energy transfer of the excited triplet. One part of $^1O_2$ could be used for the oxidative transformation of AHTN, indicating the potential risks of AHTN as a PCPs additive. And the rest of $^1O_2$ could oxidize to damage amino acids like His and Met. These results suggested that the photosensitive damage of amino acids via $^1O_2$ oxidation might be targeted and occur easily in amino acids that react readily with $^1O_2$ during the photochemical transformation of ATHN. Besides, the produced $^1O_2$ from photosensitive AHTN could effectively react with other biomolecules, such as DNA and protein. These oxidative damages have been associated with various diseases, including skin inflammation and skin cancer [49]. In addition, with the competition of $^1O_2$ consumption, the persistence of AHTN could be increased on the skin surface, causing photosensitive oxidative damage of amino acids to human skin.

3.2.2. Activator

In our system, besides the oxidation damage of amino acids from the photosensitization of AHTN, AHTN could act as an activator to react with these three amino acids during their photochemical transformation. These might be due to the interference of amino acids on electron transfer during the photochemical transformation of AHTN [32], inducing the different reactivity of AHTN with amino acids. Therefore, NBT was selected as a probe to explore the reaction of electron transfer on the photochemical transformation of AHTN with and without amino acids, during which NBT^{2+} could be reduced to form NBT^+, resulting in the increased absorbance of the mixtures at 560 nm [40]. As shown in Fig. 4, almost no absorbance at 560 nm was detected in the only presence of NBT, indicating that NBT^+ would not be spontaneously produced in the experimental system. However, the absorbance at 560 nm was increased in the mixtures of AHTN and NBT because the forming biradicals of AHTN could induce the generation of NBT^+ through electron transfer, consistent with previous studies [46,50]. In a ternary hybrid system of AHTN, amino acids, and NBT, the absorbance variation pattern at 560 nm was His > Gly > Met. These results indicate that the biradical levels of AHTN were promoted by His and weakly promoted by Gly. Besides, Met could suppress the biradical levels of AHTN due to interfering with the triplet excited state of AHTN, which was the precursor of biradicals [32]. These suggest that amino acids could affect the transient intermediate (the

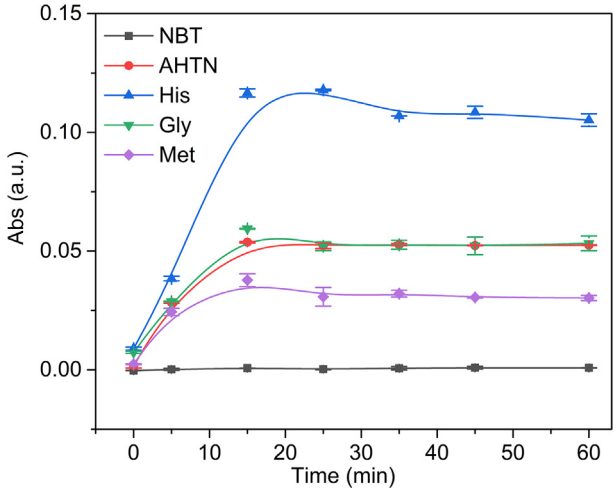

Fig. 4. Variation trend of absorbance at 560 nm with time after adding nitroblue tetrazolium (NBT) in AHTN and amino acid reaction system.

excited state of AHTN and biradicals) of AHTN photochemical transformation. Based on our previous study, these results could be induced by the N electron density of the α-amino group of amino acids [32]. Therefore, the degree of electron transfer between AHTN and amino acids in the photochemical transformation was due to the N electron density of amino acids, leading to different formation possibilities of imines.

To further explore the electron transfer relationship between the N electron density of amino acid and AHTN in photochemical transformation, quantum chemistry was employed to calculate the N charge of amino acids. Considering the pH of the human skin ranges from 4.5 to 7.5 [51,52], the α-amino group present in the same form as the $-NH_3^+$ group in His, Gly, and Met (Fig. S9), and the charge densities were charged as −0.1419, −0.1434, and −0.1392, respectively (Table S4). The N charge of His and Gly was more negative than that of Met, suggesting that electron transfer between His/Gly and AHTN was more likely to occur, which further explained the above experimental results about the promotion of biradical levels by His/Gly. Besides, His^+ and His^0 were the domain species of His as the pH = 4.5−7.5 (Proportion >98%, Fig. S9). With the increase of pH, the side-chain imidazole of His gradually transformed from a positively charged protonated imidazole group to a neutral imidazole group. Thus, electron transfer between His and AHTN was correlated with the morphology of the imidazole ion in His side chain. For the β-N of the imidazole group (Table S5), the N atom was charged from −0.1045 to −0.1515, indicating that His had more active sites for electron transfer than Gly. Therefore, the experimental and theoretical results were consistent, suggesting that AHTN photochemical transformation could easily activate the negatively charged N in amino acids via electron transfer.

Furthermore, to investigate the effect of side-chain imidazole of His (His^+ and His^0) on the photochemical transformation of AHTN, the kinetics experiments were designed at pH 4.5−7.5. As Fig. 5 shows, the pseudo-first-order rate constant of AHTN photochemical transformation was essentially invariant from pH 4.5 to 7.5, suggesting that the photochemical transformation of AHTN might be unrelated to the pH (4.5−7.5). However, the transformation rate constant of AHTN changed from 8.4×10^{-2} to $(5.0–7.6) \times 10^{-2}$ min^{-1} with the presence of His^+ and His^0, suggesting that side-chain imidazole of His could interfere with the photochemical transformation of AHTN. Besides, the transformation constant of AHTN between groups showed significant differences (Fig. 5). This was an associated result of His competition for $^1O_2$ and side-chain imidazole of His interference with electron transfer in AHTN. On the one hand, His could compete better for $^1O_2$ in an acidic environment [41]. On the other hand, the stability of imines might be affected differently due to the two N-containing groups in amino acids. According to the previous research [12], the nucleophilic addition reaction of carbonyl of AHTN and α-amino groups yielded imines accompanied by the C=N covalent bond (Fig. S10). Meanwhile, these imines possibly protonate in the acid environment and then hydrolyze into parent reactant AHTN [38]. These processes could decrease the transformation rate of AHTN in the acidic solution of His, as observed in our experiment (Fig. 5). These results could explain why the transformation rate of AHTN decreases more obviously in the acidic solution of His. Besides, as Fig. S10 shows, when C and N combine successfully, the lone pair electron repulsion of O and N caused the quaternary C to be crowded, resulting in steric hindrance, which tends to release tension from the leaving group [34,38]. All of the above results led to a tremendous challenge in identifying these by-products with the N-group of amino acid side chain and a carbonyl group. Therefore, to evaluate the reactivity of the photochemical degradation of AHTN with N-containing groups of amino acids, the quantum chemical method was applied to explore the nucleophilic addition reaction energy (ΔE) between AHTN (including AHTN photochemical transformation products) and amino acids.

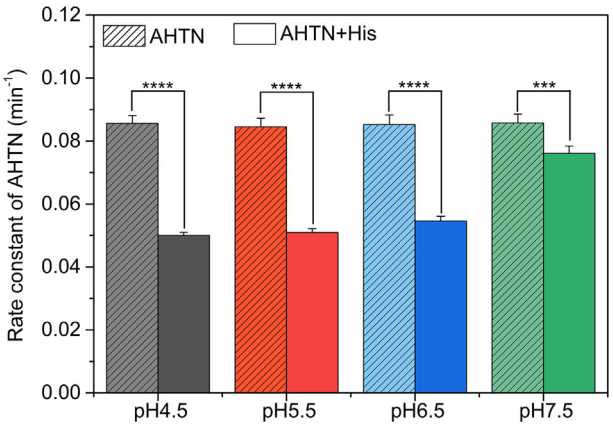

Fig. 5. At pH = 4.5, 5.5, 6.5, and 7.5, the photochemical degradation rate constants of AHTN in the presence and absence of His. Data were means of three replicates and analyzed statistically with one-way ANOVA. Statistical significance between the groups is indicated as ****$p < 0.0001$ and ***$p = 0.0005$.

As shown in Table S6−S8, except for the reaction of P3 with His, which was endothermic projection (ΔE = 0.42 kcal/mol), the ΔE values of the other reactions range were obtained from −808.23 to −43.93 kcal/mol for His, −807.31 to −2.42 kcal/mol for Gly and −806.82 to −0.23 kcal/mol for Met. These results indicate that these reactions were all easily exothermic, suggesting the photochemical degradation of AHTN could be reactive with N-containing groups of amino acids. These were probably because the α-amino group of amino acids with abundant charge density was a typical nucleophilic primary amine group, while the carbonyl group, as the characteristic group of AHTN and its transformation by-products, exhibits a high degree of polarization [38]. The electron in the carbonyl π orbital is more inclined to oxygen, resulting in the easy attack by a nucleophile, such as the α-amino group [53]. Therefore, despite the forming imines being a dynamic balance, the forward reaction also dominates this reaction at physiological pH (≈7) [34]. These theoretical results demonstrated that AHTN and its transformation by-products could readily react with amino acids to form imines.

3.3. *Skin photosensitization potency during the photochemical transformation of AHTN*

The experimental and theoretical studies above showed that imines could be generated from the reaction of AHTN and its transformation by-products with amino acids (His, Gly, and Met). Thus, the direct use of AHTN as additives in PCPs might not be as safe as previously speculated on the skin. A previous study has reported that phototoxicity of AHTN is observed in the skin of rabbits, and guinea pigs show well-defined positive results in several photosensitization tests of AHTN [54]. Therefore, these above chemical reaction processes could be considered to be the MIEs of the AOPs for skin sensitization [12]. Generally, skin photosensitization in the natural skin surface begins with a chemical event, that is, chemical sensitizers modify amino acid residues. Subsequently, skin photosensitization requires a series of biological events, including the abnormal folding of protein conformation and the activation of different cutaneous cells [55,56]. Based on this, the direct peptide reactivity assay, usually accompanied by the appearance of imines, has been employed by the Organization for Economic Co-operation and Development (OECD) to predict the sensitization potential of skin sensitizers without using test animals [38]. Therefore, the formation of imines as one of the MIE could be direct evidence of skin photosensitization during the photochemical transformation of AHTN, suggesting that AHTN was a potential skin-photosensitive damage agent under UV irradiation. Besides, in this work, from the viewpoint of the forming imines, the reaction activity of AHTN with His was higher than that of Gly and Met during AHTN photochemical degradation. This result implies that His is more important in AHTN-induced skin photosensitization.

4. Conclusions

This work has explored the potential skin sensitization mechanism of typical PCPs, AHTN, in the simulated skin surface environment, conducting both experimental and computational methods. The photochemical transformation of AHTN was investigated in the presence of amino acids, which act as an essential building block of human tissue. Amino acids could inhibit the photochemical transformation rate of AHTN, resulting in the increasing persistence of AHNT on the skin surface. Besides, the interaction between amino acids and AHTN was also attempted, finding that AHTN served dual roles as both photosensitizer and activator. As a photosensitizer, AHTN can induce the formation of $^1O_2$ to cause oxidative damage to different amino acids, indicating deterioration in the targeting of amino acids. As an activator, AHTN could react with these three amino acids (His, Gly, and Met) to form imines during their photochemical transformation via the nucleophilic addition reaction. These chemical reaction processes were considered the MIEs of the AOPs for skin sensitization. Despite the reported results of this study, there are reasons for optimism. The photochemical transformation of AHTN to skin photosensitization might not be accessible when the added dose is limited in PCPs. Besides, there is a gap between this study's system and the natural skin surface because the skin photosensitization process of photochemical transformation of AHTN might be affected by the natural skin surface proteins and cells. Thus, based on the results of this work, the interaction of AHTN and skin protein will be a subject of further attention. Overall, the interaction mechanism between AHTN and amino acids can be instructive for the skin photosensitization mechanism of AHTN. These results might explain the potential sensitizing effect of AHTN on human skin at the molecular level and provide the scientific basis for the use standard of AHTN and the development of new products in the future.

Declaration of competing interests

The authors declare no conflicts of interest.

Acknowledgments

This work was supported by the National Key Research and Development Program of China (2019YFC1804503 and 2019YFC1804501), the Key-Area Research and Development Program of Guangdong Province (2020B1111350002), the Local Innovative and Research Teams Project of Guangdong Pearl River Talents Program (2017BT01Z032), the National Natural Science Foundation of China (41977365 and 41425015), and the Key Project of Guangdong-Guangxi Joint Fund (2020B1515420002).

Appendix A. Supplementary data

Supplementary data to this article can be found online at https://doi.org/10.1016/j.eehl.2023.03.002.

References

[1] Y. Yang, Y.S. Ok, K.-H. Kim, E.E. Kwon, Y.F. Tsang, Occurrences and removal of pharmaceuticals and personal care products (PPCPs) in drinking water and water/sewage treatment plants: a review, Sci. Total Environ. 596–597 (2017) 303–320, https://doi.org/10.1016/j.scitotenv.2017.04.102.

[2] Q. Bu, B. Wang, J. Huang, S. Deng, G. Yu, Pharmaceuticals and personal care products in the aquatic environment in China: a review, J. Hazard Mater. 262 (2013) 189–211, https://doi.org/10.1016/j.jhazmat.2013.08.040.

[3] Y. Lu, T. Yuan, W. Wang, K. Kannan, Concentrations and assessment of exposure to siloxanes and synthetic musks in personal care products from China, Environ. Pollut. 159 (12) (2011) 3522–3528, https://doi.org/10.1016/j.envpol.2011.08.015.

[4] V. Homem, E. Silva, A. Alves, L. Santos, Scented traces–Dermal exposure of synthetic musk fragrances in personal care products and environmental input assessment, Chemosphere 139 (2015) 276–287, https://doi.org/10.1016/j.chemosphere.2015.06.078.

[5] K. Fournier, N. Marina, N. Joshi, V.R. Berthiaume, S. Currie, A.E. Lanterna, J.C. Scaiano, Scale-up of a photochemical flow reactor for the production of lignin-coated titanium dioxide as a sunscreen ingredient, J. Photochem. Photobiol., A 7 (2021), 100040, https://doi.org/10.1016/j.jpap.2021.100040.

[6] K.M. Hanson, E. Gratton, C.J. Bardeen, Sunscreen enhancement of UV-induced reactive oxygen species in the skin, Free Radic. Biol. Med. 41 (8) (2006) 1205–1212, https://doi.org/10.1016/j.freeradbiomed.2006.06.011.

[7] A.R. Abid, B. Marciniak, T. Pędziński, M. Shahid, Photo-stability and photo-sensitizing characterization of selected sunscreens' ingredients, J. Photochem. Photobiol. A-Chem. 332 (2017) 241–250, https://doi.org/10.1016/j.jphotochem.2016.08.036.

[8] S. Kliegman, S.N. Eustis, W.A. Arnold, K. McNeill, Experimental and theoretical insights into the involvement of radicals in triclosan phototransformation, Environ. Sci. Technol. 47 (13) (2013) 6756–6763, https://doi.org/10.1021/es3041797.

[9] E.L. Bastos, M.S. Baptista, Editorial: special issue on endogenous photosensitizers and their roles in skin photodamage and photoprotection, J. Photochem. Photobiol., A 8 (2021), 100085, https://doi.org/10.1016/j.jpap.2021.100085.

[10] H. Xu, Y. Jia, Z. Sun, J. Su, Q.S. Liu, Q. Zhou, G. Jiang, Environmental pollution, a hidden culprit for health issues, Eco-Environ. Health 1 (1) (2022) 31–45, https://doi.org/10.1016/j.eehl.2022.04.003.

[11] B. Kurz, I. Ivanova, W. Bäumler, M. Berneburg, Turn the light on photosensitivity, J. Photochem. Photobiol. 8 (2021), 100071, https://doi.org/10.1016/j.jpap.2021.100071.

[12] A. Natsch, R. Emter, Reaction chemistry to characterize the molecular initiating event in skin sensitization: a journey to Be continued, Chem. Res. Toxicol. 30 (1) (2017) 315–331, https://doi.org/10.1021/acs.chemrestox.6b00365.

[13] G. Li, X. Liu, J. An, H. Yang, S. Zhang, P.-K. Wong, T. An, H. Zhao, Photocatalytic and photoelectrocatalytic degradation and mineralization of small biological compounds amino acids at TiO_2 photoanodes, Catal. Today 245 (2015) 46–53, https://doi.org/10.1016/j.cattod.2014.05.040.

[14] G. Li, X. Liu, T. An, P.K. Wong, H. Zhao, A novel method developed for estimating mineralization efficiencies and its application in PC and PEC degradations of large molecule biological compounds with unknown chemical formula, Water Res. 95 (2016) 150–158, https://doi.org/10.1016/j.watres.2016.02.066.

[15] Y. Gao, G. Li, S. Ma, T. An, Research progress and challenge of synthetic musks: from personal care, environment pollution to human health, Prog. Chem. 29 (9) (2017) 1082–1092, 10. 7536/PC170448.

[16] A. Pinkas, C.L. Goncalves, M. Aschner, Neurotoxicity of fragrance compounds: a review, Environ. Res. 158 (2017) 342–349, https://doi.org/10.1016/j.envres.2017.06.035.

[17] J. Liu, W. Zhang, Q. Zhou, Q. Zhou, Y. Zhang, L. Zhu, Polycyclic musks in the environment: a review of their concentrations and distribution, ecological effects and behavior, current concerns and future prospects, Crit. Rev. Environ. Sci. Technol. 51 (4) (2020) 323–377, https://doi.org/10.1080/10643389.2020.1724748.

[18] R.D. Parker, E.V. Buehler, A. Newmann, Phototoxicity, photoallergy, and contact sensitization of nitro musk perfume raw materials, Contact Dermatitis 14 (2) (1986) 103–109, https://doi.org/10.1111/j.1600-0536.1986.tb01169.x.

[19] W.W. Lovell, D.J. Sanders, Photoallergic potential in the Guinea-pig of the nitromusk perfume ingredients musk ambrette, musk moskene, musk xylene, musk ketone, and musk tibetene, Int. J. Cosmet. Sci. 10 (6) (1988) 271–279, https://doi.org/10.1111/j.1467-2494.1988.tb00027.x.

[20] N. Karschuk, Y. Tepe, S. Gerlach, W. Pape, H. Wenck, R. Schmucker, K. Wittern, A. Schepky, et al., A novel in vitro method for the detection and characterization of photosensitizers, PLoS One 5 (12) (2010), 15221, https://doi.org/10.1371/journal.pone.0015221.

[21] Y. Zhang, L. Huang, Y. Zhao, T. Hu, Musk xylene induces malignant transformation of human liver cell line L02 via repressing the TGF-β signaling pathway, Chemosphere 168 (2017) 1506–1514, https://doi.org/10.1016/j.chemosphere.2016.12.001.

[22] K.M. Taylor, M. Weisskopf, J. Shine, Human exposure to nitro musks and the evaluation of their potential toxicity: an overview, Environ. Health 13 (2014) 14, https://doi.org/10.1186/1476-069X-13-14.

[23] V. Mersch-Sundermann, H. Schneider, C. Freywald, C. Jenter, W. Parzefall, S. Knasmüller, Musk ketone enhances benzo(a)pyrene induced mutagenicity in human derived Hep G2 cells, Mutat. Res., Genet. Toxicol. Environ. Mutagen. 495 (1–2) (2001) 89–96, https://doi.org/10.1016/S1383-5718(01)00202-9.

[24] C. Burns, D.A. Goldstein, Synthetic musk compounds and effects on human health? Environ. Health Perspect. 113 (2005) 800–807, https://doi.org/10.1289/ehp.7645.

[25] H. Nakata, M. Hinosaka, H. Yanagimoto, Macrocyclic-, polycyclic-, and nitro musks in cosmetics, household commodities and indoor dusts collected from Japan: implications for their human exposure, Ecotoxicol. Environ. Saf. 111 (2015) 248–255, https://doi.org/10.1016/j.ecoenv.2014.09.032.

[26] B.I. Tavera, F. Tames, J.A. Silva, S. Ramos, V. Homem, N. Ratola, H. Carreras, Biomonitoring levels and trends of PAHs and synthetic musks associated with land use in urban environments, Sci. Total Environ. 618 (2018) 93–100, https://doi.org/10.1016/j.scitotenv.2017.10.295.

[27] Z. Li, N. Yin, Q. Liu, C. Wang, T. Wang, Y. Wang, G. Qu, J. Liu, et al., Effects of polycyclic musks HHCB and AHTN on steroidogenesis in H295R cells, Chemosphere 90 (3) (2013) 1227–1235, https://doi.org/10.1016/j.chemosphere.2012.09.056.

[28] S. Schnell, R. Martion-Skilton, D. Fernandes, C. Porte, The interference of nitro- and polycyclic musks with endogenous and xenobiotic metabolizing enzymes in carp: an in vitro study, Environ. Sci. Technol. 43 (2009) 9458–9464, https://doi.org/10.1021/es902128x.

[29] J. Tumová, P. Šauer, O. Golovko, O. Koba Ucun, R. Grabic, J. Máchová, H. Kocour Kroupová, Effect of polycyclic musk compounds on aquatic organisms: a critical literature review supplemented by own data, Sci. Total Environ. 651 (2019) 2235–2246, https://doi.org/10.1016/j.scitotenv.2018.10.028.
[30] L. Wollenberger, M. Breitholtz, K. Ole Kusk, B.-E. Bengtsson, Inhibition of larval development of the marine copepod Acartia tonsa by four synthetic musk substances, Sci. Total Environ. 305 (1–3) (2003) 53–64, https://doi.org/10.1016/s0048-9697(02)00471-0.
[31] L. Till, E. David, Nitromusk and polycyclic musk compounds as long-term inhibitors of cellular xenobiotic defense systems mediated by multidrug transporters, Environ. Health Perspect. 113 (2005) 17–24, https://doi.org/10.1289/ehp.7301.
[32] H. Fang, Y. Gao, H. Wang, H. Yin, G. Li, T. An, Photo-induced oxidative damage to dissolved free amino acids by the photosensitizer polycyclic musk tonalide: transformation kinetics and mechanisms, Water Res. 115 (2017) 339–346, https://doi.org/10.1016/j.watres.2017.03.006.
[33] R.A. Lundeen, E.M. Janssen, C. Chu, K. McNeill, Environmental photochemistry of amino acids, peptides and proteins, Chimia 68 (11) (2014) 812–817, https://doi.org/10.2533/chimia.2014.812.
[34] A. Natsch, H. Gfeller, T. Haupt, G. Brunner, Chemical reactivity and skin sensitization potential for benzaldehydes: can Schiff base formation explain everything? Chem. Res. Toxicol. 25 (10) (2012) 2203–2215, https://doi.org/10.1021/tx300278t.
[35] D.W. Roberts, T.W. Schultz, A.M. Api, Skin sensitization QMM for HRIPT NOEL data: aldehyde schiff-base domain, Chem. Res. Toxicol. 30 (6) (2017) 1309–1316, https://doi.org/10.1021/acs.chemrestox.7b00050.
[36] Z. Zhang, S. Wang, L. Li, Emerging investigator series: the role of chemical properties in human exposure to environmental chemicals, Environ. Sci. Process Impacts 23 (12) (2021) 1839–1862, https://doi.org/10.1039/d1em00252j.
[37] J. Ahn, C. Avonto, A.G. Chittiboyina, I.A. Khan, Is isoeugenol a prehapten? Characterization of a thiol-reactive oxidative byproduct of isoeugenol and potential implications for skin sensitization, Chem. Res. Toxicol. 33 (4) (2020) 948–954, https://doi.org/10.1021/acs.chemrestox.9b00501.
[38] A. Bohme, J. Moldrickx, G. Schuurmann, Amino reactivity of glutardialdehyde and monoaldehydes horizontal line chemoassay profile vs skin sensitization potency, Chem. Res. Toxicol. 34 (11) (2021) 2353–2365, https://doi.org/10.1021/acs.chemrestox.1c00266.
[39] T. An, H. Fang, G. Li, S. Wang, S. Yao, Experimental and theoretical insights into photochemical transformation kinetics and mechanisms of aqueous propylparaben and risk assessment of its degradation products, Environ. Toxicol. Chem. 33 (8) (2014) 1809–1816, https://doi.org/10.1002/etc.2632.
[40] M.M. Tarpey, I. Fridovich, Methods of detection of vascular reactive species–Nitric oxide, superoxide, hydrogen peroxide, and peroxynitrite, Circ. Res. 89 (3) (2001) 224–236, https://doi.org/10.1161/hh1501.094365.
[41] P. Di Mascio, G.R. Martinez, S. Miyamoto, G.E. Ronsein, M.H.G. Medeiros, J. Cadet, Singlet molecular oxygen reactions with nucleic acids, lipids, and proteins, Chem. Rev. 119 (3) (2019) 2043–2086, https://doi.org/10.1021/acs.chemrev.8b00554.
[42] F. Wilkinson, W.P. Helman, A.B. Ross, Rate constants for the decay and reactions of the lowest electronically excited singlet state of molecular oxygen in solution. An expanded and revised compilation, J. Phys. Chem. Ref. Data 24 (2) (1995) 663–677, https://doi.org/10.1063/1.555965.
[43] E. Appiani, R. Ossola, D.E. Latch, P.R. Erickson, K. McNeill, Aqueous singlet oxygen reaction kinetics of furfuryl alcohol: effect of temperature, pH, and salt content, Environ. Sci. Process Impacts 19 (4) (2017) 507–516, https://doi.org/10.1039/c6em00646a.
[44] Y. Gao, X. Niu, M. Wang, G. Li, An, T., an inescapable fact: toxicity increase during photo-driven degradation of emerging contaminants in water environments, Curr. Opin. Green Sust. 30 (2021), 100472, https://doi.org/10.1016/j.cogsc.2021.100472.
[45] M. Cavinato, P. Jansen-Dürr, Molecular mechanisms of UVB-induced senescence of dermal fibroblasts and its relevance for photoaging of the human skin, Exp. Gerontol. 94 (2017) 78–82, https://doi.org/10.1016/j.exger.2017.01.009.
[46] N. Luo, Y. Gao, M. Wang, X. Niu, G. Li, T. An, A new bi-radical species formed during the photochemical degradation of synthetic musk tonalide in water: study of in-situ laser flash photolysis and validation of synthesized standard sample, Sci. Total Environ. 859 (2023), 160311, https://doi.org/10.1016/j.scitotenv.2022.160311.
[47] R. Alvarez-Sánchez, D. Basketter, C. Pease, J.-P. Lepoittevin, Studies of chemical selectivity of hapten, reactivity, and skin sensitization potency. 3. Synthesis and studies on the reactivity toward model nucleophiles of the 13C-labeled skin sensitizers, 5-Chloro-2-methylisothiazol-3-one (MCI) and 2-Methylisothiazol-3-one (MI), Chem. Res. Toxicol. 16 (5) (2003) 627–636, https://doi.org/10.1021/tx0256634.
[48] E.L. Schymanski, J. Jeon, R. Gulde, K. Fenner, M. Ruff, H.P. Singer, J. Hollender, Identifying small molecules via high resolution mass spectrometry: communicating confidence, Environ. Sci. Technol. 48 (4) (2014) 2097–2098, https://doi.org/10.1021/es5002105.
[49] P. Karran, R. Brem, Protein oxidation, UVA and human DNA repair, DNA Repair 44 (2016) 178–185, https://doi.org/10.1016/j.dnarep.2016.05.024.
[50] J.C. Scaiano, Temperature dependence of the photochemistry of o-methylacetophenone. A laser flash photolysis study, Chem. Phys. Lett. 73 (2) (1980) 319–322, https://doi.org/10.1016/0009-2614(80)80381-2.
[51] A. Mena-Bravo, M.D. Luque de Castro, Sweat: a sample with limited present applications and promising future in metabolomics, J. Pharm. Biomed. Anal. 90 (2014) 139–147, https://doi.org/10.1016/j.jpba.2013.10.048.
[52] P. Escobedo, C.E. Ramos-Lorente, A. Martínez-Olmos, M.A. Carvajal, M. Ortega-Muñoz, I.d. Orbe-Payá, F. Hernández-Mateo, F. Santoyo-González, et al., Wireless wearable wristband for continuous sweat pH monitoring, Sensor Actuat. B- Chem. 327 (2021), 128948, https://doi.org/10.1016/j.snb.2020.128948.
[53] D. Gleeson, M.P. Gleeson, Theoretical studies to estimate the skin sensitization potential of chemicals of the Schiff base domain, Int. J. Quant. Chem. 120 (12) (2020), 26218, https://doi.org/10.1002/qua.26218.
[54] A.M. Api, D. Belsito, D. Botelho, M. Bruze, G.A. Burton Jr., J. Buschmann, P. Calow, M.L. Dagli, et al., RIFM FRAGRANCE INGREDIENT SAFETY ASSESSMENT, 6-acetyl-1,1,2,4,4,7-hexamethyltetraline, CAS registry number 21145-77-7, Food Chem. Toxicol. 110 (1) (2017) S95–S103, https://doi.org/10.1016/j.fct.2017.03.019.
[55] D.W. Roberts, A.O. Aptula, G. Patlewicz, Mechanistic applicability domains for non-animal based prediction of toxicological endpoints. QSAR analysis of the schiff base applicability domain for skin sensitization, Chem. Res. Toxicol. 19 (9) (2006) 1228–1233, https://doi.org/10.1021/tx060102o.
[56] R.I. de Ávila, S. Carreira Santos, V. Siino, F. Levander, M. Lindstedt, K.S. Zeller, Adjuvants in fungicide formulations can be skin sensitizers and cause different types of cell stress responses, Toxicol Rep 9 (2022) 2030–2041, https://doi.org/10.1016/j.toxrep.2022.11.004.